

PAPER • OPEN ACCESS

Towards ballistic transport CVD graphene by controlled removal of polymer residues

To cite this article: Tianbo Duan *et al* 2022 *Nanotechnology* **33** 495704

View the [article online](#) for updates and enhancements.

You may also like

- [Graphene-enhanced Raman imaging of TiO₂ nanoparticles](#)
Denys Naumenko, Valentinas Snitka, Boris Snopok *et al.*
- [CVD-graphene/graphene flakes dual-films as advanced DSSC counter electrodes](#)
Andrea Capasso, Sebastiano Bellani, Alessandro Lorenzo Palma *et al.*
- [Confocal laser scanning microscopy as a real-time quality-assessment tool for industrial graphene synthesis](#)
Dong Jin Kim, Chang-Won Lee, Yeonjoon Suh *et al.*



EDINBURGH
INSTRUMENTS

WORLD LEADING
MOLECULAR
SPECTROSCOPY SOLUTIONS



edinst.com

Towards ballistic transport CVD graphene by controlled removal of polymer residues

Tianbo Duan^{1,2} , Hu Li^{1,2,3,*} , Raffaello Papadakis⁴  and Klaus Leifer^{1,*} 

¹Shandong Technology Centre of Nanodevices and Integration, School of Microelectronics, Shandong University, 250101 Jinan, People's Republic of China

²Department of Materials Science and Engineering, Ångström Laboratory, Uppsala University, SE-75121 Uppsala, Sweden

³Shenzhen Research Institute of Shandong University, 518057 Shenzhen, People's Republic of China

⁴TdB Labs, SE-75651 Uppsala, Sweden

E-mail: Hu.Li@sdu.edu.cn and Klaus.Leifer@angstrom.uu.se

Received 16 June 2022, revised 20 August 2022

Accepted for publication 29 August 2022

Published 19 September 2022



Abstract

Polymer-assisted wet transfer of chemical vapor deposited (CVD) graphene has achieved great success towards the true potential for large-scale electronic applications, while the lack of an efficient polymer removal method has been regarded as a crucial factor for realizing high carrier mobility in graphene devices. Hereby, we report an efficient and facile method to clean polymer residues on graphene surface by merely employing solvent mixture of isopropanol (IPA) and water (H₂O). Raman spectroscopy shows an intact crystal structure of graphene after treatment, and the x-ray photoelectron spectroscopy indicates a significant decrease in the C–O and C=O bond signals, which is mainly attributed to the removal of polymer residues and further confirmed by subsequent atomic force microscopy analysis. More importantly, our gated measurements demonstrate that the proposed approach has resulted in a 3-fold increase of the carrier mobility in CVD graphene with the electron mobility close to 10 000 cm² V^{−1} S^{−1}, corresponding to an electron mean free path beyond 100 nm. This intrigues the promising application for this novel method in achieving ballistic transport for CVD graphene devices.

Supplementary material for this article is available [online](#)

Keywords: chemical vapor deposited graphene, polymer removal, ballistic transport

(Some figures may appear in colour only in the online journal)

Introduction

Graphene synthesized by chemical vapor deposition (CVD) method exhibits remarkable potentialities in large-scale production of electronic nanodevices ranging from sensors [1–3], transistors [4–6] to transparent conductors [7, 8] and many more. During the essential handling procedure which transfers CVD

graphene grown on metal catalyst substrate such as Cu, Ni, etc, to insulating substrate like SiO₂/Si substrate [9–11], a polymer-assisted film acting as the supporter is necessarily employed to prevent graphene from being damaged. The most commonly used polymers in this process are poly(methyl methacrylate) (PMMA) [12–15], polycarbonates (PCs) [16, 17], and polydimethylsiloxane [18, 19], which need to be removed by solvents after transferring. However, the complete removal of the residual polymers is still challenging [20, 21]. Moreover, in the compulsory lithographic route, where graphene is fabricated into various electronic devices, polymer impurities can be introduced onto graphene [22, 23], e.g. PMMA residuals from electron beam lithography (EBL) process. As it has been investigated in a large number of studies, the residual polymers play a

* Authors to whom any correspondence should be addressed.



Original content from this work may be used under the terms of the [Creative Commons Attribution 4.0 licence](#). Any further distribution of this work must maintain attribution to the author(s) and the title of the work, journal citation and DOI.

considerably negative role in influencing the graphene performance, because they not only introduce uncertainty into the measurements of intrinsic physical properties, but also dramatically degrade the electrical properties of graphene, leading to the carrier mobility of CVD graphene on SiO₂ substrate typically in the range between 1000 and 3000 cm² V⁻¹ S⁻¹ [24]. Currently, the most frequently used method to alleviate such problem is annealing. For instance, studies have shown that annealing in a reductive atmosphere (e.g. H₂/Ar) has a positive effect on the removal of polymer residues [25–27]. Likewise, a similar effect of the annealing has also been reported both in vacuum [28–31] and inert atmospheres [32, 33]. However, most high-temperature annealing (≥ 250 °C) methods will inevitably introduce disorders in graphene structure and thus deteriorate the electrical properties of graphene [34]. Mechanical methods such as using atomic force microscopy (AFM) tips to scrape the graphene surface have also been studied albeit it is extremely low efficient and difficult to be realized in a controlled way [35–37]. Solvent treatment is the most commonly employed method to clean polymer residues. Chemical bath treatment such as using acetone, acetic acid, chloroform, and formamide can effectively remove large amount of predominant polymer residues whereas leaving a small fraction of polymers acting as doping and scattering source, which can lead to the dramatic decrease of the charge carrier mobility. Isopropanol (IPA) and water (H₂O) mixture has been proposed as an efficient developer for PMMA in EBL from the 1980s to realize high resolution fabrication of the semiconductor devices [38–40]. From there on, the effectiveness and high efficiency of this binary solvent mixture have been addressed by many researchers [41]. It is reported by Ocola [42] that both tightly bonded –OH group and non-hydrogen bonded –OH group in alcohol/H₂O mixture play a key role in the dissolution of PMMA. However, systematic investigations on the cleaning effect of IPA/H₂O on the removal of polymer residues on graphene surface have not yet been reported.

In this study, we propose a facile and effective method to achieve controlled removal of the PMMA residues on graphene by using IPA/H₂O mixture. This mixture treatment is applied as a final cleaning step after other solvent treatment and annealing. To investigate the optimized parameters, graphene samples are treated with mixtures of different volume IPA/water ratios. The surface status of the graphene is characterized by Raman spectroscopy and x-ray photoelectron spectroscopy (XPS) to exhibit the effectiveness of this method. The adhesion force mapping using AFM is used to further prove the altered physical properties of graphene after cleaning. Importantly, gated measurements are also carried out to demonstrate the significant improvement of charge carrier mobility after IPA/H₂O mixture treatment.

Results and discussion

The controlled removal of polymer residues is achieved by immersing monolayer CVD graphene on SiO₂/Si substrate into IPA/water mixture with different volume ratios as shown in figure 1(a). The volume IPA/water ratios are set to be 0% (*I*₀), 25% (*I*₂₅), 50% (*I*₅₀), 75% (*I*₇₅) and 100% (*I*₁₀₀),

respectively, to investigate the effect of volume ratio of IPA on the removal of PMMA residues. It is worth to be noted that the IPA/H₂O treatment is the final process before any other treatments (details can be found in materials and characterization). For the sample which is treated with pure water (*I*₀), it is observed in our work that the monolayer graphene is completely damaged due to the water intercalation between graphene and underneath SiO₂ substrate [43] as shown in figure S1 (available online at stacks.iop.org/NANO/33/495704/mmedia). Therefore, the sample *I*₀ is excluded in the following discussions. As a control experiment, we also prepared an untreated sample as a reference sample (*I*_{ref}). From the Raman spectra in figure 1(b), it can be clearly seen that after different treatments, the intrinsic G peaks (1585 cm⁻¹) and D peaks (1350 cm⁻¹), corresponding to the in-plane vibration mode of phonons and disorder of crystal structure, respectively, remain nearly unchanged [44–46]. This implies that the crystal structure of monolayer graphene is undamaged after treatment. In addition, we have observed a red shift up to 2.6 ± 0.8 cm⁻¹ and the decrease of full width half maximum (FWHM) up of G peak to 4.3 ± 1.9 cm⁻¹ for *I*₇₅ treatment, which suggests the decreased doping level of graphene [43, 47, 48]. To quantify the disorder of graphene samples under different treatment conditions, the intensity ratios of the D peak and the G peak (*I*_D/*I*_G) are plotted in figure S2. It can be seen that, after treatment, the variation of *I*_D/*I*_G is very small (less than 10%), indicating no extra defects introduced from the treatment. Our Raman characterization corresponds well to previous studies that the removal of polymer residues has rare effects on the Raman spectra of graphene [48, 49]. Moreover, we have noticed a downshift of G peak position to the maximum of 14.0 cm⁻¹, indicating the decreased P-type doping level of graphene [50]. This can also be regarded as evidence for the polymer residue removal by using IPA/H₂O mixture treatment. Therefore, it can be concluded that the IPA/H₂O mixture treatments have a negligible effect on the of graphene structure, which can maintain graphene intact.

To investigate the cleaning effect of the IPA/H₂O treatment, XPS was performed on various graphene samples. Figure 2 shows a comparison of the XPS C 1s peaks before and after treatment. It can be seen from figure 2(a) that, in the untreated sample, there are unambiguously four main components from the C1s peak of the CVD graphene after spectrum deconvolution, i.e. sp², sp³, C–O and C=O peaks. It is widely accepted that the C–O and C=O peaks located at 286.0 eV and 288.5 eV, respectively, are mainly ascribed to the polymer residues of PMMA during the transferring of CVD graphene [34]. Interestingly, a maximum decrease of C–O and C=O peaks is observed in *I*₇₅ with the peak intensities of the polymer residues reducing from 35.1% of reference sample to 7.2% of *I*₇₅ as shown in figure 2(b), where such ~5-fold decrease indicates the efficient removal of PMMA residues after treatment. Figure 2(c) shows the comparison of the total percentage (*C*_O) of the C–O and C=O peaks for different samples treated with various mixtures, from which the amount of PMMA residues on graphene surface can be quantified and compared. The result shows that, with the increase of the volume ratio of IPA, the oxygen concentration

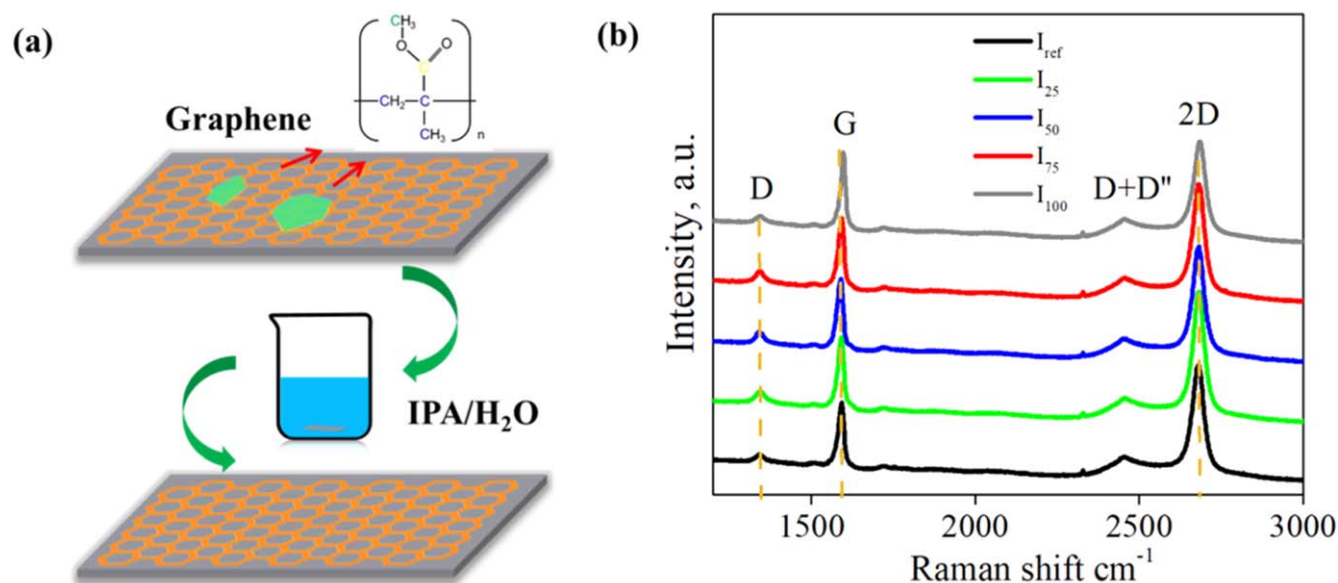


Figure 1. (a) Schematic illustration of the IPA/H₂O treatment of graphene sample on SiO₂/Si substrate. (b) Raman spectra of graphene samples with different IPA/H₂O treatment. From spectra from bottom to top are untreated reference sample, sample treated with mixtures with 25%, 50%, 75%, 100% of IPA, respectively.

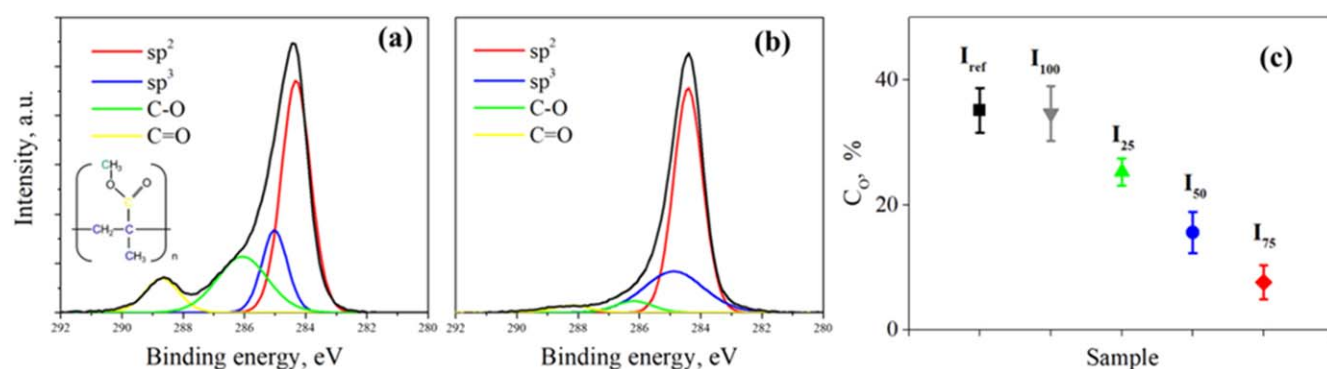


Figure 2. XPS spectra of (a) untreated sample and (b) sample I₇₅ treated with mixture of 75% IPA and 25% H₂O. (c) Concentrations of carbon oxygen bonds C_O (the add-on concentration of C-O and C=O peaks) of different samples with different IPA/H₂O treatment.

C_O has decreased to the minimum. We have found that the mixture with 75% of IPA and 25% of water is surprisingly effective in the removal of the PMMA residues, while the pure IPA has nearly no effect on the PMMA residues which also agrees with other study [51].

To further understand the polymer residue removal, we have performed surface analysis on graphene using AFM under the peakforce quantitative nanomechanical (PF-QNM) mode. Both height contrast map (figures 3(a), (d)) and adhesion contrast map (figures 3(b) and (e)) of the reference sample and mixture treated sample I₇₅ are acquired under PF-QNM mode with fixed set point of 200 nN. From the AFM comparisons of figures 3(a) and (d), it can be clearly seen that there is no significant difference in the height images of both samples which is in accordance with the surface roughness measurement shown in figure S3. However, the corresponding adhesion force has significantly decreased after treatment as shown in figures 3(b) and (e), respectively. To further quantify the adhesion between tip and surface, multiple ramping measurements have been performed on 20 random locations of the reference sample and I₇₅.

As for each ramping, the adhesion force between tip and substrate can be derived from the minimum force from the retracted curve as denoted by the dashed line in figures 3(c) and (f). We have shown that after IPA/H₂O treatment, the adhesion force has decreased from 27.3 ± 2.1 nN to 21 ± 2.5 nN. It has been reported before that the adhesion force between AFM tip and graphene sample can be enlarged by the thin layer of polymer residues on the surface [52]. Therefore, the decrease of the adhesion force after treatment provides clear evidence for the effective removal of PMMA residues on the graphene. Moreover, to further illustrate the removal of PMMA layer on graphene surface, the edge height measurement of graphene on SiO₂ has been performed. From figure S3, it can be clearly seen that the edge height has decreased from 1.32 ± 0.22 nm to 0.86 ± 0.14 nm after treatment with 75% vol. IPA/H₂O mixture, which can be attributed to the removal of PMMA. To further understand the thickness evolution of graphene after treatment, FWHM of 2D peak and intensity ratio I_{2D}/I_G , which are crucial indicators for the layer determination of graphene on substrate have also been plotted in figure S2. It can be seen that

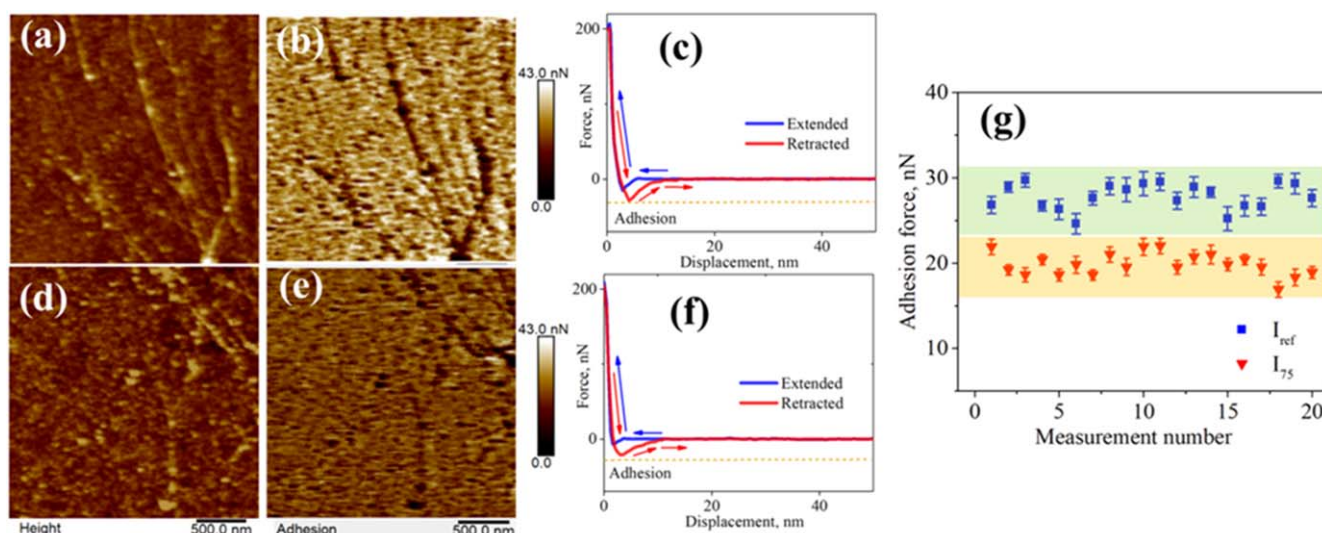


Figure 3. Atomic force microscopy characterization of after IPA/H₂O treatment: (a) and (b) show the height contrast image and corresponding adhesion mapping of untreated graphene, while (d) and (e) show the height contrast image and corresponding adhesion mapping of graphene treated with 75% IPA and 25% H₂O. (c) And (f) illustrates the representative force displacement curves of reference sample and graphene treated with 75% IPA and 25% H₂O; the adhesion force is derived from the minimum of retracted curve indicated by the dashed line. (g) Adhesion force between tip and graphene samples with error bar; the measurements are carried out on 20 different locations.

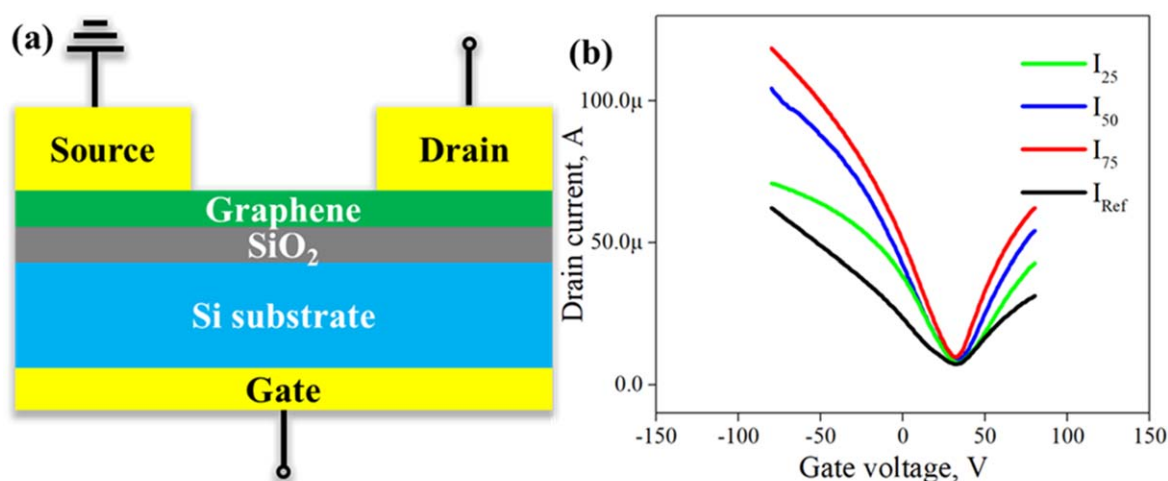


Figure 4. (a) Illustration figure of graphene back-gate transistors on SiO₂/Si with metal contacts. (b) Comparison of gated measurements on graphene samples with drain voltage of 50 mV.

the FWHM of graphene is $\sim 33 \text{ cm}^{-1}$ before treatment and reduced to $\sim 30 \text{ cm}^{-1}$ after treatment for I_{75} sample. Moreover, the I_{2D}/I_G shows a slight increase from 1.71 in I_{ref} to 1.90 in I_{75} . Both results on FWHM of 2D peak and the intensity ratio I_{2D}/I_G indicate an ideal monolayer graphene with reduced residues after cleaning using IPA/H₂O [48, 53].

It has been widely accepted that the adhesion of polymer residues on the surface is one of the key factors that undermines the ultrahigh charge carrier mobility of CVD graphene. In order to demonstrate the effectiveness of this cleaning method, we have performed gated measurements on samples with different mixture treatments. As shown in figure 4(a), typical back-gated graphene devices are fabricated by EBL with 2-probe metal contact. These devices are treated with different IPA/H₂O mixtures in accordance with the previous treatments on graphene samples. The thickness t of SiO₂ as the dielectric layer is

300 nm and the underneath P-doped Si++ is used as a back gate. The drain voltage V_{ds} is fixed to be 50 mV while the back gate voltage is varied from -80 to 80 V. Figure 4(b) shows the characteristic back-gated curves of graphene devices after different treatments. All the devices exhibit a p-doped transistor characteristic with the Dirac point located around $+30$ V, this can be mainly attributed to the doping effect from the intercalated water between graphene and substrate due to the ambient atmosphere. It is worth to be noticed that the shift of Dirac points of the graphene residues can be a crucial factor that improves the transport properties of graphene. Moreover, a statistical study on various devices using this treatment is shown in figure S4, the results suggest the high reproducibility and reliability of this facile method. Therefore, we can conclude that the charge carrier mobility can be significantly improved by the IPA/H₂O treatment as a result of PMMA removal.

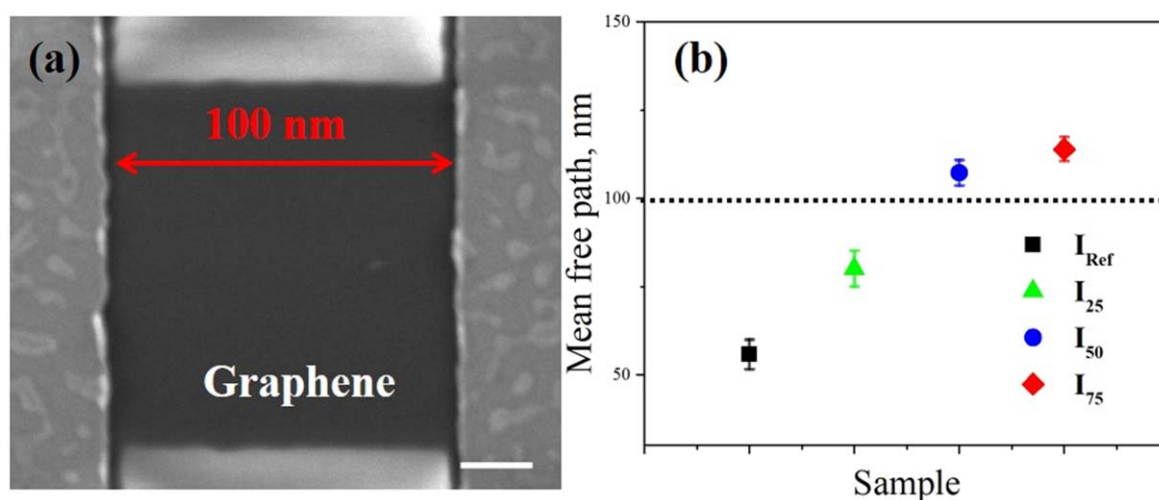


Figure 5. (a) Scanning electron microscopy image of graphene channel with 100 nm in length which is comparable to the maximum mean free path after treatment. The length of scale bar is 20 nm. (b) Mean free path of graphene treated with IPA/H₂O mixture.

Another important parameter of graphene for many electronic applications is the mean free path (MFP) λ . When λ is comparable to the channel length of electronic device, the samples after treatment with IPA/H₂O mixture is within ± 5.0 V, indicating the PMMA residues have limited doping effects on graphene sample. To further investigate the cleaning effect of the method, the electron mobility μ can be derived according to the simple parallel capacitor model [54]. We have found that with the increase of volume ratio of IPA, the mobility of graphene is increased from $3200 \text{ cm}^2 \text{ V}^{-1} \text{ S}^{-1}$ to $9650 \text{ cm}^2 \text{ V}^{-1} \text{ S}^{-1}$, which is a considerably high value in CVD graphene. We have noticed that the intrinsic CVD graphene used in this work has the mobility of $3200 \text{ cm}^2 \text{ V}^{-1} \text{ S}^{-1}$ which is comparable to many previous studies [3, 10, 34]. It is reported both theoretically and experimentally that polymer residues not only act as the scattering center [55, 56], but also would locally alter the charge carrier density of graphene. Therefore, the removal of polymer ballistic transport can be achieved. Here, we have calculated the mean free path of the graphene devices after treatment with IPA/H₂O according to Drude mode [57], and the result is shown in figure 5(b). From the comparison, it can be seen that the MFP in the normal graphene sample (I_{ref}) is less than 50 nm, while the MFPs of the IPA/H₂O treated devices exhibit an increasing trend as the volume ratio of IPA increases. The largest MFP is found up to 110 nm achieved by the mixture treatment of 75% IPA and 25% H₂O (v/v). It is worth to be pointed out that the channel length of 100 nm in graphene devices can be easily and realistically achieved by EBL as a demonstration in figure 5(a), therefore our proposed cleaning technique opens up a simple and promising way towards ballistic nanodevices for CVD graphene on SiO₂ substrate.

Materials and characterizations

Materials and device fabrications

Monolayer CVD graphene on $1 \times 1 \text{ cm}^2$ copper foil is purchased from Graphenea. The Cu foil with the thickness of

$18 \mu\text{m}$ is heated to 1000°C in H₂ atomosphere. With the introducing of 35 sccm of CH₄(g) and cool down to room temperature, the monolayer graphene is synthesized [58]. The monolayer graphene is then transferred onto a 300 nm thick SiO₂ on Si++ substrate by PMMA-assisted method. The graphene devices are fabricated by using standard EBL in Nano-beam nB5 EBL system, oxygen plasma etching in Advanced Vacuum Vision 320 reactive ion etching system, metal deposition in Lesker PVD 75 system. The detailed process of graphene transferring and EBL process can be found in supplementary information. To remove polymer residues, graphene samples are immersed into different IPA/H₂O mixture with a series of IPA volume ratios (0%, 25%, 50%, 75%, and 100%) for 5 min and followed by a N₂ blow dry. All graphene samples are treated with 1h acetone cleaning and 200°C vacuum annealing for 1 h prior to the IPA/H₂O treatment.

Characterizations

Raman and x-ray photoelectron spectra are acquired in Renishaw inVia Raman spectrometer with a 532 nm excitation laser and Physical Electronics Quantera II Scanning XPS Microprobe monochrome Al K α radiation (1486.7 eV) with a 45° angle of electron emission, respectively. Scanning electron microscopy (SEM) and light optical microscopy images are acquired in Zeiss Merlin SEM and Olympus AX70 microscope, respectively. The electrical measurements of the graphene devices are carried out using Agilent B1500 semiconductor parameter analyzer inside a Faraday cage with metal probes.

Conclusions

In conclusion, we have reported a novel method to achieve controlled removal of polymer residues on CVD graphene. The C–O and C=O signal originated from PMMA residues can be significantly reduced from 35.1% to 7.2% after treatment with

the mixture of 75% IPA and 25% H₂O. The charge carrier mobility of graphene can be improved by factor of 3, corresponding to a maximum mean free path of 110 nm which shows great potential in realizing ballistic transport of CVD graphene in the air.

Acknowledgments

Örjan Vallin from Ångström Microstructure Laboratory, Uppsala University, is acknowledged for the technical support in the device fabrication. The authors are grateful for the financial support from China Scholarship Council, Shandong Provincial Natural Science Foundation grants ZR2021QE148 and 2022HWYQ-060, Guangdong Basic and Applied Basic Research Foundation grant 2022A1515011473, Olle Engkvist grant 211-0068 and Formas grant 2019-01538.

Data availability statement

All data that support the findings of this study are included within the article (and any supplementary files).

Author contributions


Conceptualization HL; methodology, TD, HL, RP, KL, formal analysis TD, HL; data curation, TD, HL; writing—original draft preparation, TD; writing—reviewing and editing, TD, HL, RP, KL; supervision, HL and KL All authors have read and agreed to the published version of the manuscript.


Conflicts of interest

There are no conflicts to declare.

ORCID iDs

Tianbo Duan  <https://orcid.org/0000-0002-0126-9947>

Hu Li  <https://orcid.org/0000-0003-1050-8441>

Raffaello Papadakis  <https://orcid.org/0000-0001-9734-7550>

Klaus Leifer  <https://orcid.org/0000-0002-8360-1877>

References

- [1] Li H, Wani I H, Ashok A, Han Y Y, Jafri S H M, Acharya S and Leifer K 2017 Enhanced gas sensing performance of graphene/ZnS-CdS hetero-nanowires gas sensor synthesized by Langmuir–Blodgett self-assembly method *J. Phys.: Conf. Ser.* **922** 012023
- [2] Mehdi Pour M *et al* 2017 Laterally extended atomically precise graphene nanoribbons with improved electrical conductivity for efficient gas sensing *Nat. Commun.* **8** 820
- [3] Khan K, Tareen A K, Aslam M, Wang R H, Zhang Y P, Mahmood A, Ouyang Z B, Zhang H and Guo Z Y 2020 Recent developments in emerging two-dimensional materials and their applications *J. Mater. Chem. C* **8** 387–440
- [4] Lin Y-M, Jenkins K A, Valdes-Garcia A, Small J P, Farmer D B and Avouris P 2009 Operation of graphene transistors at gigahertz frequencies *Nano Lett.* **9** 422–6
- [5] Bai J, Liao L, Zhou H, Cheng R, Liu L, Huang Y and Duan X 2011 Top-gated chemical vapor deposition grown graphene transistors with current saturation *Nano Lett.* **11** 2555–9
- [6] Wei W, Deokar G, Belhaj M, Mele D, Pallecchi E, Pichonat E, Vignaud D and Happy H 2014 Fabrication and characterization of CVD-grown graphene based field-effect transistor 6–9 Oct. 2014) *44th European Microwave Conference* 367–70
- [7] Bae S, Kim H, Lee Y, Xu X, Park J-S, Zheng Y, Balakrishnan J, Lei T, Kim H R and Song Y I 2010 Roll-to-roll production of 30-inch graphene films for transparent electrodes *Nat. Nanotechnol.* **5** 574
- [8] Lee Y, Bae S, Jang H, Jang S, Zhu S-E, Sim S H, Song Y I, Hong B H and Ahn J-H 2010 Wafer-scale synthesis and transfer of graphene films *Nano Lett.* **10** 490–3
- [9] Wang Y, Zheng Y, Xu X F, Dubuisson E, Bao Q L, Lu J and Loh K P 2011 Electrochemical delamination of CVD-grown graphene film: toward the recyclable use of copper catalyst *ACS Nano* **5** 9927–33
- [10] Guo B, Xiao Q L, Wang S H and Zhang H 2019 2D Layered materials: synthesis, nonlinear optical properties, and device applications *Laser Photonics Rev.* **13** 1800327
- [11] Chaitoglou S and Bertran E 2017 Effect of temperature on graphene grown by chemical vapor deposition *J. Mater. Sci.* **52** 8348–56
- [12] Li X, Cai W, An J, Kim S, Nah J, Yang D, Piner R, Velamakanni A, Jung I and Tutuc E 2009 Large-area synthesis of high-quality and uniform graphene films on copper foils *Science* **324** 1312–4
- [13] Li X, Magnuson C W, Venugopal A, Tromp R M, Hannon J B, Vogel E M, Colombo L and Ruoff R S 2011 Large-area graphene single crystals grown by low-pressure chemical vapor deposition of methane on copper *J. Am. Chem. Soc.* **133** 2816–9
- [14] Liang X, Sperling B A, Calizo I, Cheng G, Hacker C A, Zhang Q, Obeng Y, Yan K, Peng H and Li Q 2011 Toward clean and crackless transfer of graphene *ACS Nano* **5** 9144–53
- [15] Pei J J, Yang J, Yildirim T, Zhang H and Lu Y R 2019 Many-body complexes in 2D semiconductors *Adv. Mater.* **31** 1706945
- [16] Park H J, Meyer J, Roth S and Skakalova V 2010 Growth and properties of few-layer graphene prepared by chemical vapor deposition *Carbon* **48** 1088–94
- [17] O'Hern S C, Stewart C A, Boutilier M S H, Idrobo J C, Bhaviripudi S, Das S K, Kong J, Laoui T, Atieh M and Karnik R 2012 Selective molecular transport through intrinsic defects in a single layer of CVD graphene *ACS Nano* **6** 10130–8
- [18] Jung W, Yoon T, Choi J, Kim S, Kim Y H, Kim T S and Han C S 2014 Superstrong encapsulated monolayer graphene by the modified anodic bonding *Nanoscale* **6** 547–54
- [19] Yoon T, Mun J H, Cho B J and Kim T S 2014 Penetration and lateral diffusion characteristics of polycrystalline graphene barriers *Nanoscale* **6** 151–6
- [20] Dan Y P, Lu Y, Kybert N J, Luo Z T and Johnson A T C 2009 Intrinsic response of graphene vapor sensors *Nano Lett.* **9** 1472–5
- [21] Chaitoglou S, Giannakopoulou T, Tsoutsou D, Vavouliotis A, Trapalis C and Dimoulas A 2019 Direct versus reverse vertical two-dimensional Mo₂C/graphene heterostructures

- for enhanced hydrogen evolution reaction electrocatalysis *Nanotechnology* **30** 415404
- [22] Lohmann T, von Klitzing K and Smet J H 2009 Four-terminal magneto-transport in graphene p-n junctions created by spatially selective doping *Nano Lett.* **9** 1973–9
- [23] Lee W H *et al* 2012 Simultaneous transfer and doping of CVD-grown graphene by fluoropolymer for transparent conductive films on plastic *ACS Nano* **6** 1284–90
- [24] Pirkle A, Chan J, Venugopal A, Hinojos D, Magnuson C W, McDonnell S, Colombo L, Vogel E M, Ruoff R S and Wallace R M 2011 The effect of chemical residues on the physical and electrical properties of chemical vapor deposited graphene transferred to SiO₂ *Appl. Phys. Lett.* **99** 122108
- [25] Lin Y C, Jin C H, Lee J C, Jen S F, Suenaga K and Chiu P W 2011 Clean transfer of graphene for isolation and suspension *ACS Nano* **5** 2362–8
- [26] Walter A L *et al* 2014 Luminescence, patterned metallic regions, and photon-mediated electronic changes in single-sided fluorinated graphene sheets *ACS Nano* **8** 7801–8
- [27] Leong W S *et al* 2019 Paraffin-enabled graphene transfer *Nat. Commun.* **10** 1–8
- [28] Song J, Kam F Y, Png R Q, Seah W L, Zhuo J M, Lim G K, Ho P K H and Chua L L 2013 A general method for transferring graphene onto soft surfaces *Nat. Nanotechnol.* **8** 356–62
- [29] Matsumae T, Koehler A D, Suga T and Hobart K D 2016 A scalable clean graphene transfer process using polymethylglutarimide as a support scaffold *J. Electrochem. Soc.* **163** E159–61
- [30] Auchter E, Marquez J, Yarbrough S L and Dervishi E 2017 A facile alternative technique for large-area graphene transfer via sacrificial polymer *AIP Adv.* **7** 125306
- [31] Nasir T, Kim B J, Kim K W, Lee S H, Lim H K, Lee D K, Jeong B J, Kim H C, Yu H K and Choi J Y 2018 Design of softened polystyrene for crack- and contamination-free large-area graphene transfer *Nanoscale* **10** 21865–70
- [32] Gong C *et al* 2013 Rapid Selective etching of PMMA residues from transferred graphene by carbon dioxide *J. Phys. Chem. C* **117** 23000–8
- [33] Wood J D *et al* 2015 Annealing free, clean graphene transfer using alternative polymer scaffolds *Nanotechnology* **26** 055302
- [34] Lin Y C, Lu C C, Yeh C H, Jin C H, Suenaga K and Chiu P W 2012 Graphene annealing: how clean can it be? *Nano Lett.* **12** 414–9
- [35] Goossens A M, Calado V E, Barreiro A, Watanabe K, Taniguchi T and Vandersypen L M K 2012 Mechanical cleaning of graphene *Appl. Phys. Lett.* **100** 073110
- [36] Lindvall N, Kalabukhov A and Yurgens A 2012 Cleaning graphene using atomic force microscope *J. Appl. Phys.* **111** 064904
- [37] Rosenberger M R, Chuang H J, McCreary K M, Hanbicki A T, Sivaram S V and Jonker B T 2018 Nano-‘squeegee’ for the creation of clean 2D material interfaces *ACS Appl. Mater. Inter.* **10** 10379–87
- [38] Bernstein G H, Hill D A and Liu W P 1992 New high-contrast developers for poly(methyl methacrylate) resist *J. Appl. Phys.* **71** 4066–75
- [39] Brambley D R and Bennett R H 1996 Electron-beam resist technology for GaAs microwave device fabrication *Gec-J. Res.* **13** 42–53
- [40] Mohsin M A and Cowie J M G 1988 Enhanced sensitivity in the electron-beam resist poly(methyl methacrylate) using improved solvent developer *Polymer* **29** 2130–5
- [41] Papanu J S, Hess D W, Soane D S and Bell A T 1989 Dissolution of thin poly(methyl methacrylate) films in ketones, binary ketone alcohol mixtures, and hydroxy ketones *J. Electrochem. Soc.* **136** 3077–83
- [42] Ocola L E, Costales M and Gosztola D J 2016 Development characteristics of polymethyl methacrylate in alcohol/water mixtures: a lithography and Raman spectroscopy study *Nanotechnology* **27** 035302
- [43] Lee D, Ahn G and Ryu S 2014 Two-dimensional water diffusion at a graphene-silica interface *J. Am. Chem. Soc.* **136** 6634–42
- [44] Casiraghi C 2009 Probing disorder and charged impurities in graphene by raman spectroscopy *Phys. Status Solidi-R* **3** 175–7
- [45] Malard L M, Pimenta M A, Dresselhaus G and Dresselhaus M S 2009 Raman spectroscopy in graphene *Phys. Rep.* **473** 51–87
- [46] Eckmann A, Felten A, Mishchenko A, Britnell L, Krupke R, Novoselov K S and Casiraghi C 2012 Probing the nature of defects in graphene by raman spectroscopy *Nano Lett.* **12** 3925–30
- [47] Berciaud S, Ryu S, Brus L E and Heinz T F 2009 Probing the intrinsic properties of exfoliated graphene: raman spectroscopy of free-standing monolayers *Nano Lett.* **9** 346–52
- [48] Bruna M, Ott A K, Ijas M, Yoon D, Sassi U and Ferrari A C 2014 Doping dependence of the raman spectrum of defected graphene *ACS Nano* **8** 7432–41
- [49] Suzuki S, Orofeo C M, Wang S N, Maeda F, Takamura M and Hibino H 2013 Structural instability of transferred graphene grown by chemical vapor deposition against heating *J. Phys. Chem. C* **117** 22123–30
- [50] Ferrari A C *et al* 2006 Raman spectrum of graphene and graphene layers *Phys. Rev. Lett.* **97** 187401
- [51] Lundstedt A, Papadakis R, Li H, Han Y, Jorner K, Bergman J, Leifer K, Grennberg H and Ottosson H 2017 White-light photoassisted covalent functionalization of graphene using 2-propanol *Small Methods* **1** 1700214
- [52] Liu X Z, Li Q Y, Egberts P and Carpick R W 2014 Nanoscale adhesive properties of graphene: the effect of sliding history *Adv. Mater. Interfaces* **1** 1300053
- [53] Bautista-Flores C, Sato-Berrú R Y and Mendoza D 2018 Raman spectroscopy of CVD graphene during transfer process from copper to SiO₂/Si substrates *Mater. Res. Express* **6** 015601
- [54] Li H, Duan T B, Haldar S, Sanyal B, Eriksson O, Jafri S H M, Hajjar-Garreau S, Simon L and Leifer K 2020 Direct writing of lateral fluorographene nanopatterns with tunable bandgaps and its application in new generation of moiré superlattice *Appl. Phys. Rev.* **7** 011403
- [55] Chen J H, Jang C, Adam S, Fuhrer M S, Williams E D and Ishigami M 2008 Charged-impurity scattering in graphene *Nat. Phys.* **4** 377–81
- [56] Suk J W, Lee W H, Lee J, Chou H, Piner R D, Hao Y F, Akinwande D and Ruoff R S 2013 Enhancement of the electrical properties of graphene grown by chemical vapor deposition via controlling the effects of polymer residue *Nano Lett.* **13** 1462–7
- [57] Williams J R, Low T, Lundstrom M S and Marcus C M 2011 Gate-controlled guiding of electrons in graphene *Nat. Nanotechnol.* **6** 222–5
- [58] Li X S *et al* 2009 Large-area synthesis of high-quality and uniform graphene films on copper foils *Science* **324** 1312–4